EurJIC
European Journal of Inorganic Chemistry

Research Article
doi.org/10.1002/ejic.202200626

Chemistry Europe
European Chemical Societies Publishing

www.eurjic.org

Special Collection

Investigations on the Reactivity of Copper(I) Complexes with a N_3S Thioether Ligand System

Thomas Rotärmel,[a] Pascal Specht,[a] Jonathan Becker,[a] Adam Neuba,[b] and Siegfried Schindler*[a]

Dedicated to the 90th birthday of Prof. Dr. Horst Elias.

In the active site of several copper monooxygenases, thioether residues are coordinated through the sulfur atom, e.g. dopamine-β-monooxygenase (DβM). The reaction of dioxygen with a series of copper(I) complexes with thioether groups in tripodal ligands based on either derivatives of tris(2-pyridylmethyl)amine (TMPA) or a guanidine system were investigated by low-temperature stopped-flow measurements. The formation of labile intermediates, an *end-on* superoxido complex, and μ-1,2-*trans*-peroxido copper(II) complexes were spectroscopically detected and a kinetic analysis allowed the calculation of activation parameters for these reactions supporting the postulated mechanism. Most interesting was the finding that replacing the ethyl group in the tren-guanidine derivative $(^{TMG}Et)_2(SEt^{Et})N$ with a methyl group allowed a dramatic increase in the stability of the formed superoxido copper complex. Measurements with ozone were performed in order to find an alternative way to obtain and stabilize the labile intermediates.

Introduction

Copper-mediated activation of molecular dioxygen is essential in various synthetic, industrial, and biological processes.[1] The binding of dioxygen to copper in the form of η^1-superoxido (A), peroxido (B and D), or oxido (C) complexes (Scheme 1) has been intensively studied for years because of the biological occurrence in proteins such as hemocyanin (Hc), the O_2-carrier for arthropods and mollusks,[2] and monooxygenases including dopamine-β-monooxygenase (DβM) and peptidyl-glycine-α-monooxygenase (PHM), enzymes that play a crucial role in the biogenesis of neurotransmitters and hormones.[3] In previous work, for example by Karlin, Stack, Tolman, and Itoh as well as by us, it was demonstrated that copper-dioxygen complex formation and its reactivity are highly dependent on the nature of the ligand.[4,5] Most copper-dioxygen adduct complexes reported in the literature contain ligands with nitrogen donors. However, in recent years, studies of contemporary interest in

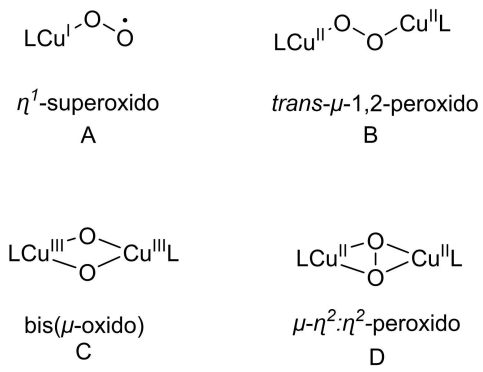

Scheme 1. Different binding modes of copper-dioxygen adducts.

Cu^I/O_2 include the influence of thioether sulfur ligation inspired by the unique active-site of the monooxygenases DβM and PHM, containing thioether ligand residues, such as cysteine (Cys) and methionine (Met).[5–7]

Therefore, several different thioether ligands have already been investigated previously.[8–10] In 2006 Karlin *et al.* described reversible copper(I)-O_2 binding and adduct formation of a *trans*-μ-1,2-peroxido dicopper(II) complex (Scheme 1, B) in a sulfur ligand environment employing a tetradentate $N_3S_{(thioether)}$ ligand, similar to the tripodal tetradentate ligand tris(2-pyridylmethyl)amine (TMPA, Scheme 2).[11,12] However, this is not a binding mode so far observed in nature. To get closer to mimicking the active site (a monomolecular *end-on*-superoxido copper complex, Scheme 1, A) of PHM,[6] Bhadra *et al.* used a thioether derivative $(^{TMG}Et)_2(SEt^{Et})N$ Scheme 2, R = Et) of the tripodal ligand tris(tetramethyl-guanidino)tren (TMG_3tren, Scheme 2). With this ligand, an *end-on*-superoxido copper complex with an experimentally proven Cu–S bond demonstrated hydrogen atom abstraction (HAA) reactivity.[13] Based on these results and

[a] T. Rotärmel, Dr. P. Specht, Dr. J. Becker, Prof. Dr. S. Schindler
Institute for Inorganic and Analytical Chemistry
Justus-Liebig-University Gießen
Heinrich-Buff-Ring 17, 35392 Gießen (Germany)
E-mail: Siegfried.schindler@ac.jlug.de
https://www.uni-giessen.de/fbz/fb08/Inst/laac/schindler
[b] A. Neuba
Department of Chemistry
University of Paderborn
Warburger Straße 100, 33098 Paderborn (Germany)

Supporting information for this article is available on the WWW under https://doi.org/10.1002/ejic.202200626

Part of the Special Collection on "Inorganic Reaction Mechanisms".

Research Article
doi.org/10.1002/ejic.202200626

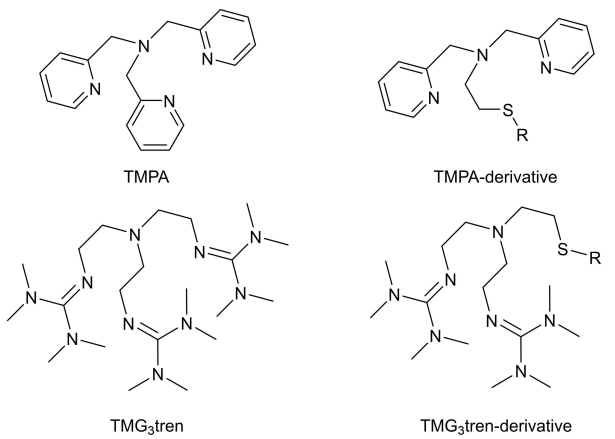

Scheme 2. Tetradentate ligands that are discussed in this work.

inspired by the biochemistry of the corresponding enzymes, we decided to investigate the role of the thioether residues in PHM and DβM by synthesizing a variety of ligand scaffolds based on the TMPA and TMG_3tren (Scheme 2) ligand system and test their reactivity towards dioxygen and ozone.

Results and Discussion

Synthesis and characterization of a copper(I) complex with a TMG_3tren-derivative

As described in the introduction, Bhadra *et al.* succeeded in mimicking the active site of the enzymes PHM and DβM.[13] However, it was necessary to perform these investigations in 2-MeTHF at −135 °C to observe the formation of the end-on superoxido complex.[13,14] We assumed that the ethyl group at the sulfur atom suppresses strong coordination to the copper(II) ion.

In the molecular structure of the copper(II) complex [(^{TMG}Et)$_2$(SEt^{Et})NCuCl]Cl the sulfur atom is not bound to the copper(II) ion most likely due to sterical reasons.[15] Therefore, it seemed likely that replacing the ethyl group with the sterically less demanding methyl group should allow the stabilization of the *end-on* superoxido complex. (^{TMG}Et)$_2$(SEt^{Me})N (Scheme 2: TMG_3tren-derivative with R = Me) was synthesized in a four-step synthesis based on the ligand synthesis of the (^{TMG}Et)$_2$(SEt^{Et})N ligand with some modifications (Scheme 3, see Experimental Section).[15] However, purification of **1** turned out tedious.

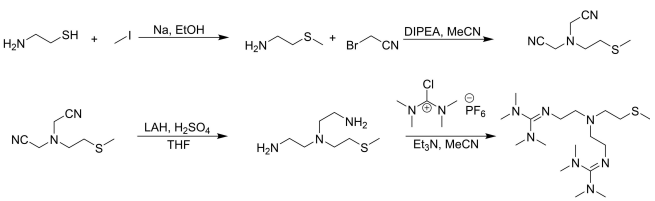

Scheme 3. Ligand Synthesis of (^{TMG}Et)$_2$(SEt^{Me})N.

During our efforts to obtain **1**, we got the ligand in the form of its sodium complex [Na(**1**)]PF_6 (the molecular structure and crystallographic data are reported in the Supporting Information 1.2). Treatment of [Na(**1**)]PF_6 with [Cu(MeCN)$_4$]PF_6 in acetone led to the isolation of a light yellow solid. Single crystals could be grown by slow solvent evaporation. As shown in Figure 1 (crystallographic data are reported in Supporting Information), the copper(I) complex could be obtained via an exchange reaction. The crystal structures revealed that the sodium and the copper complex are coordinated distorted trigonal pyramidally by three N-donor atoms and one sulfur-donor atom. The Cu–S bond length in the copper-complex (2.2684(6) Å) falls in the normal range for Cu^I–$S_{thioether}$ complexes. According to literature copper(I) complexes containing at least one thioether ligand reveal typical Cu–S bond distances between 2.20 and 2.44 Å.[16,17,18] This distorted trigonal pyramidal geometry presents an open coordination site for further ligand binding. The Cu–S (2.2684(6) Å) and Cu–N bond distances (2.0183(18), 2.0209(18), and 2.2035(17) Å) are comparable with the bond lengths of the copper complex with (^{TMG}Et)$_2$(SEt^{Et})N (Cu–S 2.2709(5), Cu–N 2.0362(15), 2.0436(15) and 2.1987(14) Å).[13] The molecular structures of the copper(II) complexes [(**1**)CuCl]Cl and [(**1**)CuCl]BPh_4 have been reported previously and show that in the solid state the sulfur atom is coordinated, supporting our findings.[19]

Oxygenation reactions of [Cu(1)]PF_6

Quite surprisingly, [Cu^I(**1**)]$^+$ with different anions tetrakis(3,5-bis(trifluoromethyl)phenyl)borate ([$BAr^F{}_4$]$^-$ and tetrakis(pentafluorophenyl)borate B(C_6F_5)$_4^-$) did not dissolve in 2-MeTHF, so that a direct comparison with the reaction of [(^{TMG}Et)$_2$(SEt^{Et})NCu]B(C_6F_5)$_4$ with dioxygen under identical conditions was not possible. However, [Cu^I(**1**)]PF_6 could be reacted with dioxygen in acetone at −90 °C (Scheme 4). Bubbling dioxygen through a cooled complex solution led to the formation of a dark green colored solution under these conditions indicating the formation of an *end-on* superoxido complex. This was confirmed by the UV-vis spectrum of this compound which is characterized by an absorbance maximum

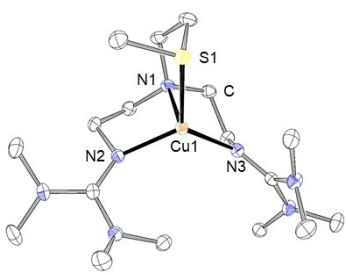

Figure 1. ORTEP representation of the copper complex described in the molecular structures of [Cu(**1**)]$^+$. H atoms and counter ion were omitted for clarity, anisotropic displacement ellipsoids were plotted at 50% probability. Selected bond lengths (Å): Cu1-S1: 2.268, Cu1-N1: 2.204, Cu1-N2: 2.018, Cu1-N3: 2.021. Selected bond angles (°): N1-Cu1-S1: 89.09, N1-Cu1-N2: 84.59, N2-Cu1-N3: 119.78, N3-Cu1-S1: 123.29.

Research Article
doi.org/10.1002/ejic.202200626

Chemistry Europe
European Chemical Societies Publishing

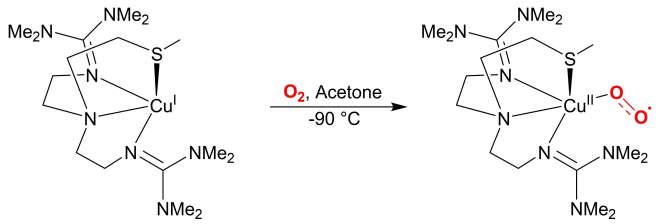

Scheme 4. Oxygenation reaction of the copper(I) complex to the end-on copper(II) superoxido complex.

at 432 nm (Figure 2) and is similar to the ethyl-derivative (442 nm) and the N_4-analog (442 nm).[13,20] In contrast, the reaction of dioxygen with $[(^{TMG}Et)_2(SEt^{Et})NCu]OTf$ in acetone did not allow the observation of the end-on superoxido complex.[15]

To gain more information about the improved stability of the end-on superoxido complex $[Cu^{I}(\mathbf{1})O_2]PF_6$ low-temperature stopped-flow measurements were performed. Time-resolved UV-vis spectra (Figure 3) were collected in acetone between

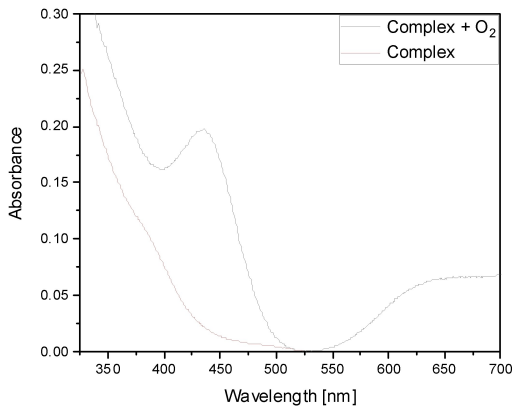

Figure 2. UV-vis spectrum of $[Cu^{I}(\mathbf{1})]PF_6$ ($c_{complex}$ = 0.75 mmol/L, red line) and after the reaction with dioxygen at −90 °C (black line).

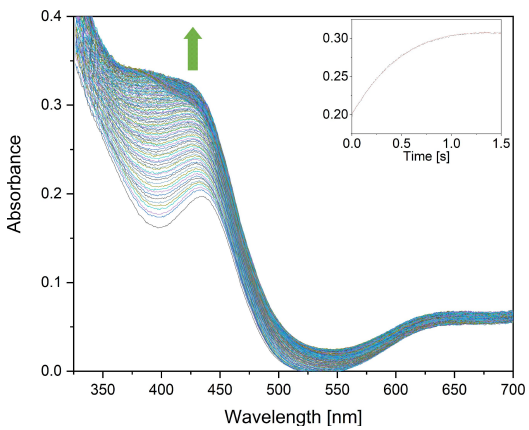

Figure 3. Time-resolved UV-vis spectra of the reaction of dioxygen ($c_{dioxygen} = 5.7 \cdot 10^{-3}$ mol/L)[22] with $[Cu^{I}(\mathbf{1})]PF_6$ in acetone ($c_{complex}$ = 0.75 mmol/L after mixing) at −90 °C. The inset displays the time dependent change in absorbance at 432 nm (black: experimental, red: exponential fit).

−90 °C and −75 °C. Measurements were performed under pseudo first order conditions ($[O_2] \gg$ [complex]) and the formation of the absorbance band at 432 nm over time could be fitted to a single exponential function, indicating first order for the complex concentration in the rate law. A plot of k_{obs} vs. dioxygen concentration showed a linear dependence with an intercept (see Supporting Information), indicating first order in $[O_2]$ and reversibility of the reaction (see Supporting Information). An Eyring plot based on the second order rate constants (see Supporting Information) allowed to calculate activation parameters $\Delta H^{\neq} = 4.9 \pm 1$ kJ·mol^{-1} and $\Delta S^{\neq} = -164 \pm 1$ J·mol^{-1}K^{-1}. The negative activation entropy indicates an associative mechanism in line with previous results. Stopped-flow measurements in acetonitrile were performed as well to investigate the stability of the *end-on* superoxido copper complex at higher temperatures. However, no reaction was observed at −40 °C in acetonitrile with dioxygen. Additionally, the reaction of ozone with $[Cu^{I}(\mathbf{1})]PF_6$ in acetone showed the same reaction as with dioxygen under the same conditions. Nearly the same behavior had been observed for the reaction of $[Cu(tet\ b)]PF_6$ with dioxygen and ozone reported previously by us.[21] Unfortunately and in contrast to the quite stable copper superoxido complex with the TMG_3tren ligand, the complex $[Cu^{II}(\mathbf{1})O_2]PF_6$ started to decompose immediately after its formation and therefore, no additional experiments were performed with this system.

Synthesis and characterization of copper(I/II) complexes with TMPA- and related derivatives

With regard to our success to stabilize the superoxido complex with a thioether derivative of TMG_3tren described above by simply replacing the ethyl group in $[(^{TMG}Et)_2(SEt^{Et})NCu]^+$ with a methyl group we decided to extend this approach to the TMPA ligand system. Previous work by Karlin and co-workers already had shown the importance and influence of the ligand design. The first synthetic attempts to obtain an *end-on*-superoxido copper complex with a modified TMPA ligand (Scheme 5, R = Et), however, had led to the formation of a binuclear μ-1,2-*trans*-peroxido dicopper(II) complex as described in the introduction.[8,18] Redesign and modification of their previous investigated N_3S ligand systems resulted in the formation of a mononuclear *end-on* superoxido copper complex in the presence of a thioether.[9]

The preparation of selected thioether-amine N_3S ligands used for the present study was performed according to the literature and is reported in the Experimental Section (Scheme 6).[8] Several ligands with two pyridyl groups and different thioether residues were synthesized. The thioether residue was modified from R = Me (Scheme 5, **2**) to sterically more demanding groups R (Scheme 5, **3**–**6**).

The reaction of **2** with $[Cu^{I}(MeCN)_4]PF_6$ in acetone as well as in dichloromethane led to the precipitation of a yellow colored solid in high yields. The formation of $[Cu^{I}(\mathbf{2})]PF_6$ was confirmed by electrospray ionization mass spectrometry (ESI-MS), revealing the characteristic peak at m/z = 336.0594 for the $[Cu^{I}(\mathbf{2})]^+$

Research Article
doi.org/10.1002/ejic.202200626

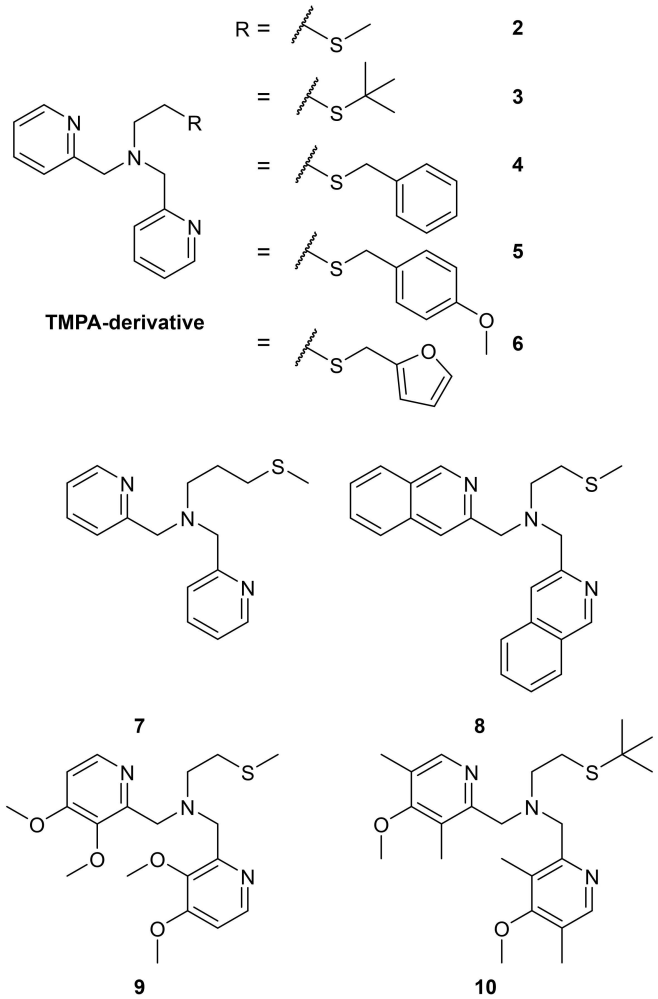

Scheme 5. Modification of the TMPA-derivative with different thioether- and pyridine-residues.

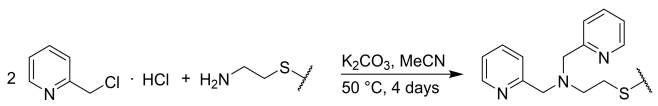

Scheme 6. Ligand Synthesis of different TMPA-derivatives.

cation. Furthermore, suitable single crystals for X-ray structural characterization were obtained. The molecular structure revealed the complex as a dimer, $[Cu^{I}(\mathbf{2})]_2(PF_6)_2$ in the solid state, where each copper ion is coordinated distorted tetrahedrally by one ligand via the three N-donors and by the other ligand via its thioether donor atom (Figure 4a). While this type of complex dimerization in the solid state has been already observed for a number of three- and four-coordinated complexes with a thioether residue,[18,23] the formation of a mononuclear form was often only indicated in solution by NMR measurements.[8]

We were able to obtain the corresponding mononuclear species in an unusual and somewhat unexpected way. The copper(I) complex had been reacted with sulfur to prepare a disulfido or trisulfido complex as described previously, however, no sulfido complex was obtained.[24] Instead $[Cu^{I}(\mathbf{2})]PF_6$ presented in Figure 4b was obtained (crystallographic data are reported in the Supporting Information) and revealed that the copper(I)-ion has a distorted trigonal-pyramidal geometry with three N-donor atoms and one sulfur-donor atom in the coordination sphere. Following the same synthetic protocol, four further ligands (Scheme 5) were synthesized. A central feature of these ligands was the introduction of more sterically demanding thioether residues with *tert*-butylthioether (in **3**), benzylthioether (in **4**), 4-methoxybenzylthioether (in **5**), and furylmethylthioether (in **6**). With these ligands, only the copper(I) complex $[Cu^{I}(\mathbf{3})]_2(BPh_4)_2$ could be crystallized (Supporting Information) and the molecular structure of this dimer is similar to that of $[Cu^{I}(\mathbf{2})]_2(PF_6)_2$. Complexes $[Cu^{I}(\mathbf{5})]_2(BPh_4)_2$ and $[Cu^{I}(\mathbf{6})]_2(OTf)_2$ were characterized by ESI-MS and elemental analysis.

Copper(II) complexes with ligands **2**, **3** and **4** could be structurally characterized, no suitable crystals with ligands **5** and **6** could be obtained. The molecular structures of $[Cu^{II}(\mathbf{2})Cl]PF_6$ (Figure 4c), $[Cu^{II}(\mathbf{3})Cl]OTf$ and $[Cu^{II}(\mathbf{4})Cl]PF_6$ (crystallographic data are reported in the Supporting Information) revealed a chloride anion as an additional ligand. This is a consequence of well-known chloride abstraction quite often observed by a reaction of copper(I) complexes with dichloromethane.[25] The crystal structure of $[Cu^{II}(\mathbf{2})Cl]PF_6$ (Figure 4c) revealed a distorted square pyramidal coordination geometry with the thioether group in an axial position with a Cu–S bond distance of 2.7418(6) Å for $[Cu^{II}(\mathbf{2})Cl]PF_6$ (Figure 4), 2.7171(7) for $[Cu^{II}(\mathbf{3})Cl]OTf$ and 2.7174(5) Å for $[Cu^{II}(\mathbf{4})Cl]PF_6$. The Cu–S bond distances are comparable with data reported previously for structurally characterized $[Cu^{II}(\mathbf{2})(Cl)](BF_4)$ by Rorabacher and co-workers who furthermore investigated redox potentials, kinetics of complex formation, and catalytic catechol oxidations.[17,26] While ligands **1**–**6** only differ in the type of thioether residues, the effect of chelate ring size was studied with ligand **7** (Scheme 5). The influence of modifications of the pyridine residue was investigated furthermore by applying ligands **8**, **9**, and **10** (Scheme 5). Reaction of the ligands **7** and **8** with copper(I)salts in an acetone/dichloromethane mixture caused the formation of yellow-colored solids, formulated as $[Cu^{I}(\mathbf{7})]BPh_4$ and $[Cu^{I}(\mathbf{8})]PF_6$, on the basis of crystal structure analysis (crystallographic data are reported in the Supporting Information). In comparison with previously described structures, the complexes turned out to be mononuclear with a Cu–S bond of 2.2031(6) and 2.2297(5) Å. Copper(II) complexes suitable for crystallographic characterization were not obtained. In contrast to copper(I) complexes with these two ligands it was not possible to obtain copper(I) complexes with ligands **9** and **10**. During the reaction of these two ligands with different copper(I) salts, a disproportionation reaction occurred and only the corresponding copper(II) complexes could be isolated. However, it was possible to crystallize the copper(II) complexes by slow solvent evaporation (the molecular structures and the crystallographic data are presented in the Supporting Information). No secondary weak interactions in the crystal structures were detected.

Research Article
doi.org/10.1002/ejic.202200626

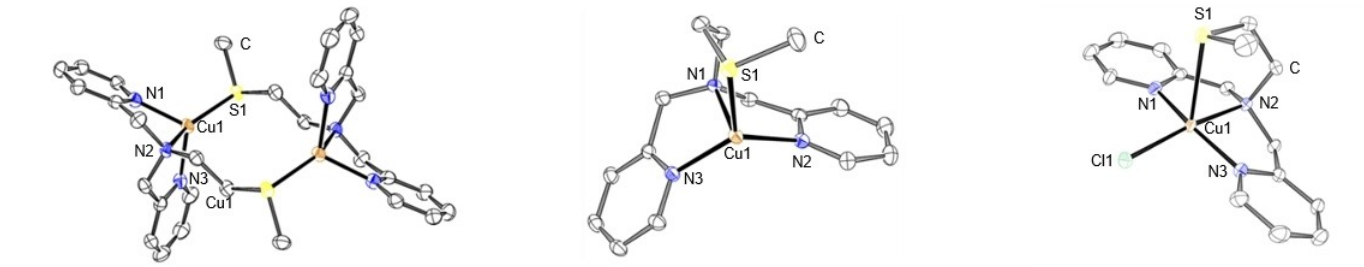

Figure 4. ORTEP representations of the dimeric Cu(I) complex (a), the monomeric Cu(I) complex (b) and the monomeric Cu(II) complex (c) described in the molecular structures of (a) $[Cu^{I}(\mathbf{2})]^{+}{}_{2}$, (b) $[Cu^{I}(\mathbf{2})]^{+}$ and (c) $[Cu^{II}(\mathbf{2})Cl]^{+}$. H atoms and counter ions were omitted for clarity, anisotropic displacement ellipsoids were plotted at 50% probability. Selected bond lengths (Å) for (a): Cu1-S1: 2.184, Cu1-N1: 2.048, Cu1-N2: 2.173, Cu1-N3: 2.047. Selected bond angles (°) for (a): S1-Cu1-N1: 119.03, N1-Cu1-N2: 80.96, N2-Cu1-N3: 82.35, N3-Cu1-S1: 122.33. Selected bond lengths (Å) for (b): Cu1-S1: 2.257, Cu1-N1: 2.203, Cu1-N2: 2.002, Cu1-N3: 2.020. Selected bond angles (°) for (b): S1-Cu1-N1: 91.44, N1-Cu1-N2: 82.40, N2-Cu1-N3: 121.84, N3-Cu1-S1: 116.83. Selected bond lengths (Å) for (c): Cu1-S1: 2.742, Cu1-N1: 1.976, Cu1-N2: 2.049, Cu1-N3: 1.987, Cu1-Cl1: 2.243. Selected bond angles (°) for (c): S1-Cu1-N1: 84.63, S1-Cu1-N2: 84.37, S1-Cu1-N3: 104.48, S1-Cu1-Cl1: 102.91, N1-Cu1-N2: 84.11, N2-Cu1-N3: 82.35, N3-Cu1-Cl1: 94.64, Cl1-Cu1-N1: 97.51.

Electrochemical studies

The copper(I) complexes were characterized by cyclic voltammetry to gain more information on the influence of the different thioether residues with regard to their redox potentials. The redox potentials were determined at a complex concentration of 2 mM in acetonitrile under anaerobic conditions starting from the copper(I) complex. Ferrocene was used as standard ($E_{1/2} = 0.65$ V under these conditions). The cyclic voltammograms for the complexes with the ligands **2**–**5** are presented in Figure 5 while cyclic voltammograms of the complexes with the ligands **6**–**10** are reported in the Supporting Information. Redox potentials are reported in Table 1. All complexes (with the exception of $[Cu(\mathbf{7})]BPh_4$ and $[Cu(\mathbf{10})]BPh_4$) showed reversible behavior and the potentials of nearly all copper(I) complexes are quite similar with a value of $E_{1/2}$ close to 0.1 V. However, the half-wave potentials of complexes with the ligands **2**–**6** indicate that sterically more demanding residues (except for **4**) result in a higher value of $E_{1/2}$. While the larger distance of the N-donor atom and the S-donor atom in Ligand **7** and the additional substitution of the pyridyl-groups in ligand **10** caused irreversibility, the modification of only the pyridyl groups with sterically demanding groups resulted in a shift to more positive oxidation values. The value of $E_{1/2}$ for the complex with ligand **2** is comparable to the results obtained by Rorabacher and co-workers in 1999. In contrast to our work, they determined the potential in an aqueous solution with ferroin as an external standard. Nevertheless changing the methyl group to the sterically more demanding ethyl group led to a higher $E_{1/2}$ value as well.[17]

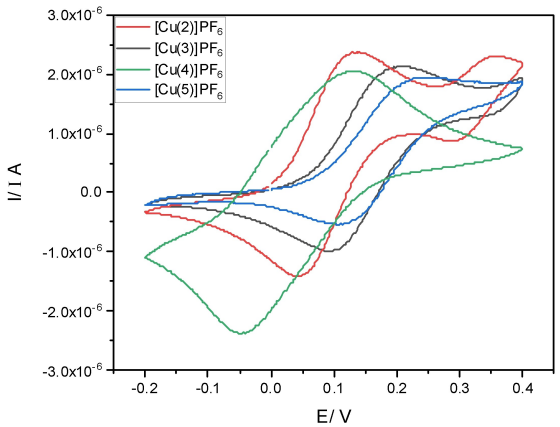

Figure 5. Cyclic voltammograms of the copper(I) complexes with ligands **2**, **3**, **4** and **5** in acetonitrile ($c_{complex} = 2$ mmol/L; $c_{electrolyte} = 0.1$ mol/L).

Table 1. Potentials of the copper(I) complexes.

Complex]	E_p^{red} [V]	E_p^{ox} [V]	$E_{1/2}$ [V]	ΔE [mV]
$[Cu(\mathbf{2})]BPh_4$	0.044	0.140	0.092	96
$[Cu(\mathbf{3})]BPh_4$	0.094	0.200	0.147	106
$[Cu(\mathbf{4})]BPh_4$	−0.050	0.130	0.040	180
$[Cu(\mathbf{5})]BPh_4$	0.114	0.250	0.182	136
$[Cu(\mathbf{6})]BPh_4$	0.204	0.326	0.265	122
$[Cu(\mathbf{7})]BPh_4$	–	–	–	–
$[Cu(\mathbf{8})]BPh_4$	0.134	0.250	0.192	116
$[Cu(\mathbf{9})]BPh_4$	−0.030	0.100	0.035	130
$[Cu(\mathbf{10})]BPh_4$	–	–	–	–

Oxygenation reactions of copper(I) complexes

As described in the introduction a number of $N_3S_{(thioether)}$ ligands, containing two pyridyl-, one amine- and one thioether-donor, have been investigated previously and showed that Cu^{I}/O_2 reactivity often led to the formation of μ-1,2-*trans*-peroxido dicopper(II) species.[8,12,18] However, further modifications of the ligand system by Karlin and co-workers allowed to generate a mononuclear copper(II) superoxido complex possessing a thioether ligation.[9]

When copper(I) complexes with ligands **2**–**6** were reacted with dioxygen, here as well, only the formation of the corresponding μ-1,2-*trans*-peroxido dicopper(II) complexes could be spectroscopically observed. Thus dioxygen reacts with $[Cu^{I}(\mathbf{3})]^{+}$ in acetone at −90 °C, forming the dark blue colored μ-1,2-*trans*-peroxido dicopper(II) species (Scheme 8).

Time resolved UV-vis spectra are presented in Figure 6. Absorbance maxima at 455 nm, 541 nm and 616 nm are consistent with the formation of the peroxido complex similar

Research Article
doi.org/10.1002/ejic.202200626

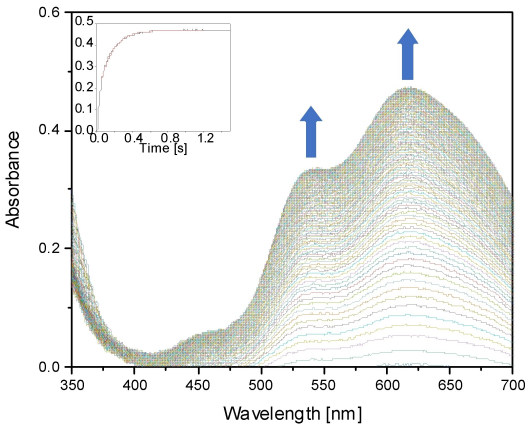

Figure 6. Time-resolved UV-vis spectra of the reaction of dioxygen ($c_{dioxygen} = 5.7 \cdot 10^{-3}$ mol/L)[22] with $[Cu^{I}(\mathbf{3})]BPh_4$ in acetone ($c_{complex} = 0.2$ mmol/L after mixing) at −90 °C. The inset displays the time dependent change in absorbance at 616 nm (black: experimental, red: exponential fit).

to other *trans*-peroxido complexes, for example [((Cu^{II}-(TMPA))$_2$(μ-1,2-O$_2$)] reported previously.[11] However, as can be seen in Figure 6, no formation of an *end-on* superoxido copper complex could be detected.

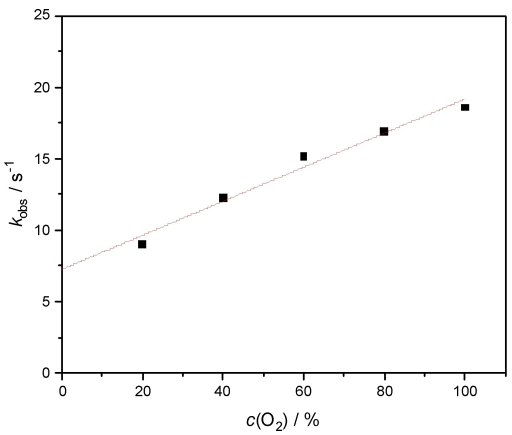

Figure 7. k_{obs} vs. $c(O_2)$ at −80 °C.

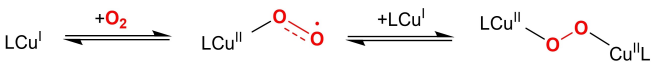

Scheme 7. Formation of the μ-1,2-*trans*-peroxido dicopper(II) species via a mononuclear copper(II) superoxido complex.

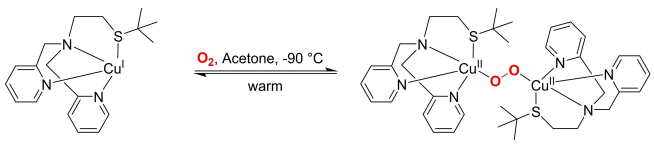

Scheme 8. Reversible dioxygen binding of $[Cu^{I}(\mathbf{3})]BPh_4$.

The absorbance vs. time trace at 616 nm (as well as at other wavelengths) obtained under pseudo first order conditions could be fitted to a one exponential function, indicating first order for the complex concentration in the rate law. A plot of k_{obs} vs. [O_2] showed a linear dependence in line with first order of dioxygen concentration as well (Figure 7). The intercept is the consequence of the reversibility of the reaction. The overall reaction sequence can be described according to Scheme 7.

While it is sometimes possible to observe the superoxido complex as an intermediate,[27] this is not the case if the formation of this species is rate-determining (followed by a very fast consecutive step). A description of the kinetics of this type of mechanism has been described previously in great detail.[28]

An Eyring plot (Figure 8) allowed the calculation of the activation parameters to $\Delta H^{\neq} = 21 \pm 1$ kJ mol^{-1} and $\Delta S^{\neq} = -70 \pm 3$ J mol^{-1} K^{-1} and is in line with previous measurements of related complexes. The negative activation entropy indicates an associative mechanism. Kinetic measurements were also performed for complexes $[Cu^{I}(\mathbf{4})]^{+}$ and $[Cu^{I}(\mathbf{6})]^{+}$ (Supporting Information) and activation parameters could be obtained (Table 2). Due to the similarity of all these reactions no detailed kinetic investigations were performed for complexes $[Cu^{I}(\mathbf{2})]^{+}$ and $[Cu^{I}(\mathbf{5})]^{+}$.

Further reactions with dioxygen were performed at −140 °C in 2-MeTHF/THF which also only allowed to spectroscopically detect the formation of the dinuclear peroxido copper complex.

Previously, we observed that ozone could be applied to generate an *end-on* superoxido copper complex.[21] Therefore, ozone was reacted with $[Cu^{I}(\mathbf{3})]^{+}$ in acetone at −90 °C. While there was an indication that a superoxido complex might have formed briefly it was not possible to really detect and character-

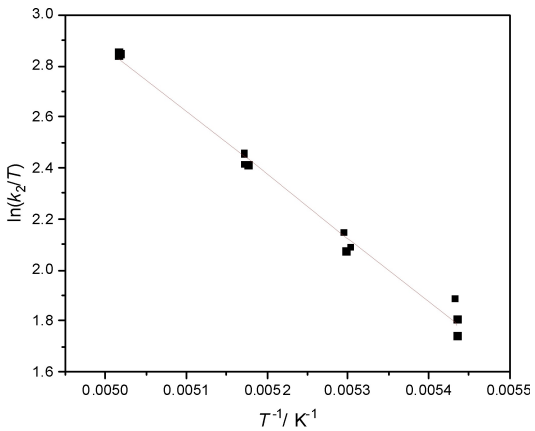

Figure 8. Eyring plot for k_2 values obtained from the temporal evolution of the absorbance at 616 nm between −89 °C and −73 °C for the reaction of $[Cu^{I}(\mathbf{3})]BPh_4$ with O_2 in acetone.

Table 2. Calculated activation parameters for the O_2-interaction in acetone at −90 °C.

Parameter[a]	$[Cu^{I}(\mathbf{3})]^{+}$	$[Cu^{I}(\mathbf{4})]^{+}$	$[Cu^{I}(\mathbf{6})]^{+}$
$\Delta H^{\neq}$ (kJ·mol^{-1})	+21 ± 1	+29 ± 1	+21 ± 1
$\Delta S^{\neq}$ (J·mol^{-1} K^{-1})	−70 ± 3	−29 ± 4	−66 ± 4

Research Article
doi.org/10.1002/ejic.202200626

ize this species. Switching the solvent to 2-MeTHF/THF and lowering the temperature to −140 °C allowed the observation of the formation of a dark green colored species followed by an immediate color change to dark blue right afterwards. While the green color strongly indicates the formation of an *end-on* superoxido copper complex, attempts to analyze this species failed due to the instability of the compound. The UV-vis spectrum of the dark blue species with absorbance maxima at 540 and 616 nm (Figure 9) are in line with the formation of the μ-1,2-*trans*-peroxido dicopper(II) complex.

The interaction of [Cu(**9**)]$^+$ and [Cu(**10**)]$^+$ with dioxygen (in acetone) and ozone (in 2-MeTHF/THF) could not be analyzed due to the fact that both complexes tend to disproportionate.

In comparison to these complexes, the copper(I) complexes of **7** and **8** did not react with dioxygen at all. The addition of O_2 at low temperature led to no spectroscopic changes and even at room temperature no color change was observed, indicating that a seemingly minor ligand modification (larger distance between the N-donor and S-donor atom in **7** and addition of a steric more demanding pyridyl group in **8**), effects the Cu^IO_2 chemistry and stability of these complexes highly.

Summary and Conclusion

The results reported herein demonstrate the importance and influence of ligand design and ligand modification in Cu^I/O_2-chemistry. Copper(I) complexes with ligands based on TMPA (= tris(2-pyridylmethyl)amine) behaved quite differently. While some complexes could not even be studied due to disproportionation in solution, other ones (e. g. due to larger chelate rings leading to a stabilization of Cu(I) complexes) did not react at all with dioxygen. In contrast, other complexes of the investigated series did form μ-1,2-*trans*-peroxido dicopper(II) that could be spectroscopically observed at low temperatures in stopped-flow measurements. However, in none of these reactions, it was possible to observe an *end-on* superoxido copper complex prior to the consecutive reaction to the peroxido complex. Kinetic measurements showed that the formation of the superoxido complex is rate-determining and therefore, it was not possible to detect this species. Differently from previous investigations by us, reactions with ozone did not provide any advantage for the systems studied here. A dark green colored species was observed in one reaction with ozone at −140 °C, however, this species was extremely short-lived and only the dark blue colored μ-1,2-*trans*-peroxido complex, formed immediately afterward, could be spectroscopically detected.

However, most interesting was the finding that replacing the ethyl group in the tren-guanidine derivative ($^{TMG}Et)_2(SEt^{Et})N$ with a methyl group allowed a dramatic increase in the stability of the superoxido copper complex that only could be observed with ($^{TMG}Et)_2(SEt^{Et})N$ at −135 °C in contrast to the −90° C (or even a bit higher) with ($^{TMG}Et)_2(Set^{Me})N$. This is important for further investigations to apply copper complexes in selective oxygenation reactions.

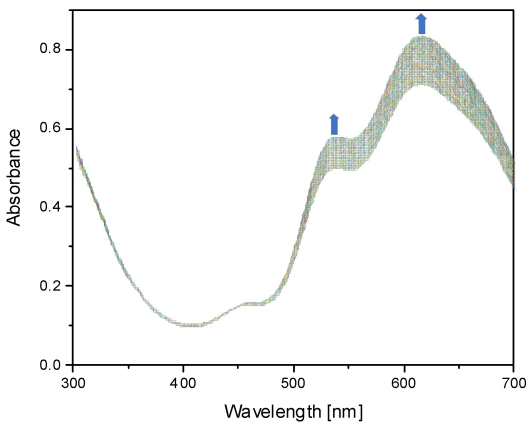

Figure 9. UV-vis spectra of the reaction of [Cu^I(**3**)]BPh_4 with ozone in 2-MeTHF/THF at −140 °C.

Experimental Section

General: All reagents and solvents used were of p.a. quality and were purchased from Sigma Aldrich and AcrosOrganics. The solvents were purified by distillation with a drying agent by standard procedures. The air sensitive syntheses of the metal complexes were performed under inert conditions in a glove box by MBraun (H_2O and O_2 concentrations less than 0.1 ppm) under an argon atmosphere. Stopped-flow measurements were carried out with a HI-Tech SF-61SX2 and CSF-61DX2 low-temperature stopped-flow unit equipped with a diode array spectrophotometer. Kinetic data were analyzed with the software Kinetic Studio (TgK Scientific). NMR measurements were performed with a Bruker Avance II 400 MHz (AV II 400). The NMR analysis of the copper(I) complexes were carried out on a Bruker Avance Neo 700 NMR spectrometer. For Electrospray-ionization MS (ESI-MS) measurements a Bruker microTOF mass spectrometer was used. UV/Vis spectra were recorded with an Agilent 8453 spectrometer. The CHN elemental analysis was performed using the CHN-Analysator: Thermo FlashEA – 1112 Series.

Electrochemistry: Cyclic voltammetry measurements were performed with a glassy carbon electrode as working electrode, a platinum/titanium electrode (counter electrode) and an Ag/AgCl reference electrode. MeCN was used as solvent and NBu_4BF_4 was applied as conducting salt. Ferrocene was used as standard ($E_{1/2}$ = 0.65 V) and the electrochemical data were recorded with an e-corder 410 edaq (eDAQ, Colorado Springs, US) and the program eChem.

Crystallography: Experimental data by single-crystal X-ray diffraction measurements were collected using a Bruker D8 Venture system, equipped with dual IμS-sources (Mo/Cu), a PHOTON 100 or PHOTON II detector and an Oxford Cryostream 700 low temperature system. More detailed information regarding crystallographic results is reported in the Supporting Information.

Deposition Numbers 2193634 (for [Cu(**1**)](PF_6)), 2195195 (for [Cu_2(**2**)$_2$]$(PF_6)_2$), 2193628 (for [Cu(**2**)](PF_6)), and 2193625 (for [Cu(**2**)Cl](PF_6)) contain the supplementary crystallographic data for this paper. These data are provided free of charge by the joint Cambridge Crystallographic Data Centre and Fachinformationszentrum Karlsruhe Access Structures service.

Research Article
doi.org/10.1002/ejic.202200626

Synthesis of Ligands

2-(Methylthio)ethanamine: To a solution of Na (4.92 g, 214 mmol) in ethanol (300 mL) 2-aminoethanethiol (15.0 g, 194 mmol) was added and stirred at room temperature for 15 min Iodomethane (29.0 g, 204 mmol) was added dropwise at 0 °C to the suspension. The reaction mixture was stirred 15 min at room temperature. Afterwards, the mixture was heated under reflux for 3 h and after cooling, distilled water (100 mL) was added. Ethanol was removed under reduced pressure and the aqueous phase was washed with dichloromethane (3×100 mL). The organic phase was dried over Na_2SO_4 and the solvent was evaporated under reduced pressure. The resulting yellow oil was purified by Kugelrohr distillation to give a colorless oil (14.6 g, 0.160 mol, 83 % yield). ^{1}H NMR (400 MHz, $CDCl_3$): δ (ppm) = 2.89 (dd, J = 6.7, 5.9 Hz, 2H), 2.60 (dd, J = 6.7, 5.9 Hz, 2H), 2.10 (s, 3H), 1.64 (s, 2H); ^{13}C NMR (100 MHz, $CDCl_3$): δ (ppm) = 40.3 (CH_2), 38.2 (CH_2), 15.1 (CH_3). HRMS (ESI): *m/z* calcd for $C_3H_{10}NS^+$: 92.0529; found: 92.0525 $[M+H]^+$; $C_3H_9NNaS^+$: 114.0348; found: 114.0357 $[M+Na]^+$.

2,2′-((2-(Methylthio)ethyl)azanediyl)diacetonitrile: To a suspension of 2-(Methylthio)ethaneamine (7.30 g, 80.1 mmol) and diisopropylethylamine (20.7 g, 160 mmol) in acetonitrile bromoacetonitrile (19.2 g, 160 mmol) was added dropwise at 0 °C. Afterwards, the reaction mixture was heated to 60 °C for 3 h. After cooling to room temperature, distilled water (100 mL) was added and the solution was extracted with dichloromethane (3×50 mL). The collected organic phases were dried over Na_2SO_4 and the solvent was removed under reduced pressure. The brown oil was extracted with warm diethylether (3×100 mL) and the ether phases were dried over Na_2SO_4. The solvent was removed under reduced pressure to give a yellow oil (7.63 g, 45.1 mmol, 56 % yield). ^{1}H NMR (400 MHz, $CDCl_3$): δ (ppm) = 3.69 (s, 4H), 2.94–2.90 (m, 2H), 2.69–2.65 (m, 2H), 2.16 (s, 3H); ^{13}C NMR (100 MHz, $CDCl_3$): δ (ppm) = 114.2 (q), 52.6 (CH_2), 42.2 (CH_2), 31.6 (CH_2), 15.8 (CH_3). HRMS (ESI): *m/z* calcd for $C_7H_{11}N_3NaS^+$: 192.0566; found: 192.0572 $[M+Na]^+$.

N′-(Aminomethyl)-N′-(2-(methylthio)ethyl)ethane-1,2-diamine: To a suspension of $LiAlH_4$ (9.75 g, 257 mmol) in dry THF (200 mL) at 0 °C conc. H_2SO_4 (12.6 g, 128 mmol) was added carefully. After addition of conc. H_2SO_4 the suspension was stirred for 30 min at 0 °C. Afterwards, 2,2′-((2-(Methylthio)ethyl)azanediyl)diacetonitrile (7.25 g, 42.8 mmol) was added dropwise to the suspension and stirred for 24 h at room temperature. Distilled water was added carefully at 0 °C to the suspension until no further gas development was observed. The suspension was filtered and the collected precipitate was washed with THF (200 mL). The solvent was evaporated under reduced pressure. The oil was treated with distilled water (100 mL) and washed with dichloromethane (3× 50 mL). The organic phases were dried over Na_2SO_4 and the solvent was removed under reduced pressure to give a yellow oil (2.22 g, 12.5 mmol, 29 %). ^{1}H NMR (400 MHz, $CDCl_3$): δ (ppm) = 2.75 (dd, J = 6.5, 5.3 Hz, 4H), 2.72–2.66 (m, 2H), 2.64–2.58 (m, 2H), 2.53 (dd, J = 6.5, 5.3 Hz, 4H), 2.12 (s, 3H), 1.47 (s, 4H); ^{13}C NMR (100 MHz, $CDCl_3$): δ (ppm) 57.3 (CH_2), 53.5 (CH_2), 39.9 (CH_2), 32.6 (CH_2), 15.8 (SCH_3). HRMS (ESI): *m/z* calcd for $C_7H_{20}N_3S^+$: 178.1373; found: 178.1385 $[M+H]^+$; $C_7H_{19}N_3NaS^+$: 200.1192; found: 200.1202 $[M+Na]^+$.

2′,2′-(((2-(Methylthio)ethyl)azanediyl)bis(ethane-2,1-diyl))bis-(1,1,3,3-tetramethyl-guanidine = 1): To an solution of N′-(Aminomethyl)-N′-(2-(methylthio)ethyl)ethane-1,2-diamine (0.50 g, 2.8 mmol) and trimethylamine (0.57 g, 5.6 mmol) in dry acetonitrile (50 mL) at 0 °C a solution of Chloro-N,N,N′,N′-tetramethylformamidinium hexa-fluorophosphate (1.6 g, 5.6 mmol) in dry acetonitrile was added dropwise. The reaction mixture was stirred 3 h under reflux. Afterwards, a solution of NaOH (0.27 g, 5.6 mmol) in distilled water (5.6 mL) was added and the solvent was evaporated under pressure. In order to deprotonate the bis-hydrochloride, KOH (50 wt.-%, 50 mL) was added and the ligand was extracted into the acetonitrile phase (3×25 mL). The collected organic phases were dried over Na_2SO_4 and the solvent was evaporated under reduced pressure to give a yellow oil (0.910 g, 1.68 mmol, 60 %). ^{1}H NMR (400 MHz, CD_3CN): δ (ppm) = 3.18–3.12 (m, 4H), 2.75–2.72 (m, 14H), 2.71–2.70 (m, 2H), 2.68 (s, 12H), 2.49–2.44 (m, 4H), 2.11 (s, 3H); ^{13}C NMR (100 MHz, CD_3CN): δ (ppm) 163.1 (q), 57.4 (CH_2), 53.9 (CH_2), 47.6 (CH_2), 39.4 (NCH_3), 31.7 (CH_2), 14.2 (SCH_3). HRMS (ESI): *m/z* calcd for $C_{17}H_{39}N_3NaS^+$: 396.2880; found: 396.2872 $[M+Na]^+$.

General ligand-synthesis: The (Chloromethyl)pyridine backbone, the thioether residue and potassium carbonate were placed in a Schlenk flask and were dissolved in dry acetonitrile (100 mL). The reaction mixture was stirred for four days under argon at 50–60 °C. After four days, the solvent was removed and the yellow oil was dissolved in dichloromethane (100 mL). The organic phase was washed three times with water (20 mL). After drying over $MgSO_4$, the solution was filtered and the solvent was removed by rotary evaporation. The yellow raw product was purified by column chromatography. The general procedure is based on the ligand synthesis of *^{DMM}ESE* published previously by Karlin and co-workers.[8] Applied amounts of reactants, purification, yields and analyses are listed for each ligand.

Bis(2-pyridylmethyl)-2-(methylthio)ethylamine (2): 2-(Chloromethyl)pyridine hydrochloride (0.500 g, 3.05 mmol), 2-(methylthio)ethylamine (0.132 g, 1.45 mmol) and potassium carbonate (2.11 g, 15.3 mmol). The yellow raw product was purified by column chromatography (alumina, 100 % ethyl acetate, R_f = 0.48) yielding a yellow oil (0.277 g, 1.01 mmol, 70 % yield). ^{1}H NMR (400 MHz, $CDCl_3$): δ (ppm) = 8.45 (ddd, J = 4.9, 1.8, 0.9 Hz, 2H), 7.59 (td, J = 7.6, 1.8 Hz, 2H), 7.51 (dt, J = 7.8, 1.2 Hz, 2H), 7.08 (ddd, J = 7.4, 4.9, 1.3 Hz, 2H), 3.80 (s, 4H), 2.78–2.71 (m, 2H), 2.65–2.57 (m, 2H), 1.95 (s, 3H); ^{13}C NMR (100 MHz, $CDCl_3$) δ (ppm) = 158.4 (q), 148.0 (CH), 135.7 (CH), 122.0 (CH), 121.0 (CH), 59.2 (CH_2), 52.4 (CH_2), 30.8 (CH_2), 14.7 (CH_3). HRMS (ESI): *m/z* calcd for $C_{15}H_{20}N_3S^+$: 274.1373; found: 274.1370 $[M+H]^+$, $C_{15}H_{19}N_3NaS^+$: 296.1192; found: 296.1200 $[M+Na]^+$.

Bis(2-pyridylmethyl)-2-(*tert*-butylthio)ethylamine (3): 2-(Chloromethyl)pyridine hydrochloride (1.35 g, 8.25 mmol), 2-(*tert*-Butylthio)ethylamine (0.500 g, 3.75 mmol) and potassium carbonate (3.11 g, 22.5 mmol). The yellow raw product was purified by column chromatography (alumina, 100 % ethyl acetate, R_f = 0.53) yielding a yellow oil (0.680 g, 2.15 mmol, 57 % yield). ^{1}H NMR (400 MHz, $CDCl_3$): δ (ppm) = 8.52 (ddd, J = 4.9, 1.8, 1.0 Hz, 2H), 7.66 (td, J = 7.6, 1.8 Hz, 2H), 7.58 (dt, J = 7.8, 1.2 Hz, 2H), 7.14 (ddd, J = 7.3, 4.8, 1.3 Hz, 2H), 3.87 (s, 4H), 2.87–2.75 (m, 2H), 2.75–2.65 (m, 2H), 1.26 (s, 9H); ^{13}C NMR (100 MHz, $CDCl_3$) δ (ppm) = 159.5 (q), 149.0 (CH), 123.0 (CH), 122.0 (CH), 121.0 (CH), 60.4 (CH_2), 54.5 (CH_2), 42.0 (q), 31.0 (CH_3), 26.0 (CH_2). HRMS (ESI): *m/z* calcd for $C_{18}H_{26}N_3S^+$: 316.1842; found: 316.1838 $[M+H]^+$.

Bis(2-pyridylmethyl)-2-(benzylthio)ethylamine (4): 2-(Chloromethyl)pyridine hydrochloride (1.69 g, 10.3 mmol), 2-(Benzylthio)ethylamine hydrochloride (0.951 g, 4.67 mmol) and potassium carbonate (3.87 g, 28.0 mmol). The yellow raw product was purified by column chromatography (alumina, 1:1 ethyl acetate/hexane, R_f = 0.56) yielding a yellow oil (0.890 g, 2.55 mmol, 55 % yield). ^{1}H NMR (400 MHz, $CDCl_3$): δ (ppm) = 8.51 (ddd, J = 4.9, 1.8, 0.9 Hz, 2H), 7.57 (td, J = 7.7, 1.8 Hz, 2H), 7.54 (dt, J = 7.8, 1.2 Hz, 2H), 7.29–7.18 (m, 5H), 7.14 (ddd, J = 7.4, 4.9, 1.3, 2H), 3.81 (s, 4H), 3.61 (s, 2H), 2.83–2.72 (m, 2H), 2.65–2.54 (m, 2H); ^{13}C NMR (100 MHz, $CDCl_3$) δ (ppm) = 159.5 (q), 149.0 (q), 138.4 (CH), 136.4 (CH), 128.8 (CH), 128.5 (CH), 127.0 (CH), 123.0 (CH), 122.0 (CH), 60.4 (CH_2), 53.6 (CH_2), 36.3 (CH_2), 28.9 (CH_2). HRMS (ESI): *m/z* calcd for $C_{21}H_{24}N_3S^+$:

350.168; found: 350.163 $[M+H]^+$, $C_{21}H_{23}N_3NaS^+$: 372.1505; found: 372.1511 $[M+H]^+$.

Bis(2-pyridylmethyl)-2-((4-methoxybenzyl)thio)ethylamine (5): 2-(Chloromethyl)pyridine hydrochloride (0.386 g, 2.35 mmol), 2-((4-Methoxybenzyl)thio)ethylamine hydrochloride (0.250 g, 1.07 mmol) and potassium carbonate (0.887 g, 6.42 mmol). The yellow raw product was purified by column chromatography (alumina, 3:1 ethyl acetate/methanol, $R_f = 0.50$) yielding a yellow oil (0.151 g, 0.398 mmol, 37% yield). ^{1}H NMR (400 MHz, $CDCl_3$): δ (ppm) = 8.44 (ddd, $J = 4.9$, 1.8, 0.9 Hz, 2H), 7.57 (td, $J = 7.6$, 1.8 Hz, 2H), 7.47 (dt, $J = 7.9$, 1.1 Hz, 2H), 7.11–7.01 (m, 4H), 6.74–6.69 (m, 2H), 3.74 (s, 4H), 3.71 (s, 3H), 3.50 (s, 2H), 2.73–2.66 (m, 2H), 2.55–2.48 (m, 2H); ^{13}C NMR (100 MHz, $CDCl_3$) δ (ppm) = 158.5 (q), 157.5 (q), 148.0 (q), 135.7 (CH), 129.4 (CH), 128.8 (CH), 122.0 (CH), 121.0 (CH), 112.8 (CH), 59.2 (CH_2), 54.2 (CH_2), 52.6 (CH_2), 34.6 (CH_2), 27.8 (CH_3). HRMS (ESI): *m/z* calcd for $C_{22}H_{26}N_3OS^+$: 380.1792; found: 380.1788 $[M+H]^+$.

Bis(2-pyridylmethyl)-2-(furfurylthio)ethylamine (6): 2-(Chloromethyl)pyridine hydrochloride (0.676 g, 4.12 mmol), 2-(Furfurythio)ethylamine (0.296 g, 1.88 mmol) and potassium carbonate (1.56 g, 11.3 mmol). The yellow raw product was purified by column chromatography (alumina, 100% ethyl acetate, $R_f = 0.13$) yielding a yellow oil (0.360 g, 1.06 mmol, 56% yield). ^{1}H NMR (400 MHz, $CDCl_3$): δ (ppm) = 8.52 (ddd, $J = 4.9$, 1.8, 0.9 Hz, 2H), 7.66 (td, $J = 7.6$, 1.8 Hz, 2H), 7.56 (dt, $J = 7.9$, 1.2 Hz, 2H), 7.30 (dd, $J = 1.9$, 0.9 Hz, 1H), 7.15 (ddd, $J = 7.5$, 4.9, 1.3 Hz, 2H), 6.25 (dd, $J = 3.2$, 1.9 Hz, 1H), 6.08 (dd, $J = 3.1$, 0.9 Hz, 1H), 3.84 (s, 4H), 3.62 (s, 2H), 2.82–2.74 (m, 2H), 2.73–2.64 (m, 2H); ^{13}C NMR (100 MHz, $CDCl_3$) δ (ppm) = 159.4 (q), 151.6 (q), 149.0 (CH), 142.1 (CH), 136.5 (CH), 123.3 (CH), 123.0 (CH), 122.1 (CH), 110.4 (CH), 107.5 (CH), 60.1 (CH_2), 53.5 (CH_2), 29.2 (CH_2), 28.3 (CH_2). HRMS (ESI): *m/z* calcd for $C_{19}H_{22}N_3OS^+$: 340.1479; found: 340.1485 $[M+H]^+$, $C_{19}H_{21}NaN_3OS^+$: 362.1298; found: 362.1300 $[M+Na]^+$.

Bis(2-pyridylmethyl)-3-(methylthio)propylamine (7): 2-(Chloromethyl)pyridine hydrochloride (3.43 g, 20.9 mmol), 3-(methylthio)propylamine (1.00 g, 9.51 mmol) and potassium carbonate (7.89 g, 57.1 mmol). The yellow raw product was purified by column chromatography (alumina, 100% ethyl acetate, $R_f = 0.54$) yielding a yellow oil (0.910 g, 3.16 mmol, 33% yield). ^{1}H NMR (400 MHz, $CDCl_3$): δ (ppm) = 8.53 (ddd, $J = 4.9$, 1.8, 0.9 Hz, 2H), 7.66 (td, $J = 7.6$, 1.8 Hz, 2H), 7.53 (d, $J = 7.8$ Hz, 2H), 7.15 (ddd, $J = 7.5$, 4.9, 1.3 Hz, 2H), 3.85 (s, 4H), 2.67 (t, $J = 7.1$ Hz, 2H), 2.52–2.42 (m, 2H), 2.04 (s, 3H), 1.84 (p, $J = 7.3$ Hz, 2H); ^{13}C NMR (100 MHz, $CDCl_3$) δ (ppm) = 159.6 (q), 149.0 (CH), 136.4 (CH), 123.0 (CH), 122.0 (CH), 60.5 (CH_2), 53.3 (CH_2), 32.0 (CH_2), 26.7 (CH_2), 15.4 (CH_3). HRMS (ESI): *m/z* calcd for $C_{16}H_{22}N_3S^+$: 288.1529; found: 288.1528 $[M+H]^+$.

Bis(2-quinolylmethyl)-2-(methylthio)ethylamine (8): 2-(Chloromethyl)quinoline hydrochloride (1.77 g, 8.25 mmol), 2-(methylthio)ethylamine (0.342 g, 3.75 mmol) and potassium carbonate (3.11 g, 22.5 mmol). The yellow raw product was purified by column chromatography (alumina, 1:1 ethyl acetate/hexane, $R_f = 0.61$) yielding a yellow solid (0.798 g, 2.14 mmol, 57% yield). ^{1}H NMR (400 MHz, $CDCl_3$): δ (ppm) = 8.14 (dd, $J = 8.5$, 0.8 Hz, 2H), 8.04 (dq, $J = 8.4$, 0.9 Hz, 2H), 7.84–7.74 (m, 4H), 7.68 (ddd, $J = 8.4$, 6.9, 1.5 Hz, 2H), 7.50 (ddd, $J = 8.1$, 6.9, 1.2 Hz, 2H), 4.07 (s, 4H), 2.90 (dd, $J = 8.5$, 6.0 Hz, 2H), 2.73 (dd, $J = 8.3$, 5.9 Hz, 2H), 1.97 (s, 3H); ^{13}C NMR (100 MHz, $CDCl_3$) δ (ppm) = 160.2 (q), 147.5 (CH), 136.4 (CH), 129.4 (CH), 129.0 (CH), 127.5 (CH), 127.4 (CH), 126.2 (CH), 121.2 (CH), 61.2 (CH_2), 53.5 (CH_2), 31.9 (CH_2), 15.7 (CH_3). HRMS (ESI): *m/z* calcd for $C_{23}H_{24}N_3S^+$: 374.1686; found: 374.1692 $[M+H]^+$, $C_{23}H_{23}N_3NaS^+$: 396.1505; found: 396.1511 $[M+Na]^+$.

Bis(3,4-dimethoxy-2-pyridylmethyl)-2-methylthioethylamine (9): 2-(Chloromethyl)-3,4-dimethoxypyridine hydrochloride (1.85 g, 8.25 mmol), 2-(methylthio)ethylamine (0.342 g, 3.75 mmol) and potassium carbonate (3.11 g, 22.5 mmol). The yellow raw product was purified by column chromatography (alumina, 1:1 ethyl acetate/hexane, $R_f = 0.61$) yielding a yellow solid (0.798 g, 2.14 mmol, 57% yield). ^{1}H NMR (400 MHz, $CDCl_3$): δ (ppm) = 8.39 (d, $J = 5.7$ Hz, 2H), 6.92 (d, $J = 5.7$ Hz, 2H), 4.17 (s, 4H), 3.94 (s, 6H), 3.83 (s, 6H), 3.09–3.01 (m, 2H), 2.77–2.70 (m, 2H), 2.02 (s, 3H); ^{13}C NMR (100 MHz, $CDCl_3$) δ (ppm) = 159.4 (q), 150.4 (CH), 144.8 (CH), 144.4 (CH), 107.5 (CH), 61.1 (CH_2), 56.0 (CH_2), 53.6 (CH_3), 53.2 (CH_3), 30.9 (CH_2), 15.4 (CH_3). HRMS (ESI): *m/z* calcd for $C_{19}H_{28}N_3O_4S^+$: 394.1796; found: 394.1801 $[M+H]^+$.

Bis(4-methoxy-3,5-dimethyl–2-pyridylmethyl)-2-(*tert*-butylthio)ethyl-amine (10): 2-(Chloromethyl)-4-methoxy-3,5-dimethylpyridine hydrochloride (0.916 g, 4.12 mmol), 2-(*tert*-Butylthio)ethylamine (0.251 g, 1.88 mmol) and potassium carbonate (1.56 g, 11.3 mmol). The yellow raw product was purified by column chromatography (alumina, 100% ethyl acetate, $R_f = 0.52$) yielding a yellow oil (0.800 g, 1.85 mmol, 98% yield). ^{1}H NMR (400 MHz, $CDCl_3$): δ (ppm) = 8.08 (s, 2H), 3.69 (s, 4H), 3.65 (s, 6H), 2.68–2.60 (m, 2H), 2.55–2.46 (m, 2H), 2.15 (s, 6H), 2.06 (s, 6H), 1.12 (s, 9H); ^{13}C NMR (100 MHz, $CDCl_3$) δ (ppm) = 163.0 (q), 156.0 (CH), 147.3 (CH), 125.4 (CH), 124.2 (CH), 58.7 (CH_2), 53.8 (CH_2), 40.9 (CH_2), 30.1 (CH_3), 24.4 (CH_2), 12.2 (CH_3), 9.7 (CH_3). HRMS (ESI): *m/z* calcd for $C_{24}H_{38}N_3O_2S^+$: 432.2680; found: 432.2675 $[M+H]^+$; $C_{24}H_{37}N_3NaO_2S^+$: 454.2499; found: 454.2500 $[M+Na]^+$.

Synthesis of Copper(I) Complexes

[Cu(1)]PF_6: To a stirred solution of **1** (0.059 g, 0.11 mmol) in 2-MeTHF (2 mL) a solution of $[Cu(MeCN)_4]PF_6$ (0.037 g, 0.10 mmol) in 2-MeTHF (2 mL) was added dropwise. The mixture was stirred over night at room temperature. Slow evaporation of the solvent led to yellow crystals that were suitable for X-ray structural characterization. Yield: 46.5 mg (0.080 mmol, 80%). ^{1}H NMR (700 MHz, acetone-*d6*): δ (ppm) = 3.25 (ddd, $J = 13.9$, 7.0, 3.8 Hz, 2H), 3.13 (ddd, $J = 13.9$, 6.9, 3.9 Hz, 2H), 2.94 (dd, $J = 9.2$, 2.8 Hz, 4H), 2.84–2.81 (m, 2H), 2.80–2.77 (m, 2H), 2.69 (s, 12H), 2.67 (s, 12H), 2.06 (s, 3H). HRMS (ESI): *m/z* calcd for $C_{17}H_{39}CuF_6N_7PS^+$: 581.1925; found: 581.1932 $[M+L]^+$. Anal. calcd (%) for $C_{17}H_{39}CuF_6N_7PS \cdot 2.5\ CH_3CN$: C 29.48, H 5.58, N 12.34, found: C 29.06, H 5.22, N 12.73.

[Cu(2)]PF_6: To a stirred solution of **2** (0.050 g, 0.18 mmol) in acetone (2 mL) a solution of $[Cu(MeCN)_4]PF_6$ (0.068 g, 0.18 mmol) in acetone (2 mL) was added dropwise. The mixture was stirred over night at room temperature. Slow evaporation of the solvent led to yellow crystals that were suitable for X-ray structural characterization. Yield: 74.4 mg (0.155 mmol, 85%). ^{1}H NMR (700 MHz, acetone-*d6*): δ (ppm) = 7.93 (s, 2H), 7.16 (s, 4H), 7.14–7.10 (m, 2H), 4.19 (s, 4H), 3.13 (s, 4H), 1.95 (s, 3H). HRMS (ESI): *m/z* calcd for $C_{15}H_{19}CuN_3S^+$: 336.0591; found: 336.0594 $[M+L]^+$. Anal. calcd (%) for $C_{15}H_{19}CuF_6N_3PS$: C 37.39, H 3.97, N 8.72, found: C 37.88, H 3.85, N 8.44.

[Cu(3)]BPh_4: To a stirred solution of **3** (0.050 g, 0.16 mmol) in dichloromethane (2 mL) a solution of $[Cu(MeCN)_4]PF_6$ (0.058 g, 0.157 mmol) in dichloromethane (2 mL) was added dropwise. After stirring for 2 h, solid $NaBPh_4$ (0.054 g, 0.16 mmol) was added and it was stirred over night at room temperature. The yellow solution was filtered and slow evaporation of the solvent led to colorless crystals that were suitable for X-ray structural characterization. Yield: 76.6 mg (0.110 mmol, 70%).^{1}H NMR (700 MHz, acetone-*d6*): δ (ppm) = 7.78 (t, $J = 7.7$ Hz, 2H), 7.48–7.38 (m, 4H), 7.21 (dddt, $J = 8.0$, 5.5, 2.8, 1.5 Hz, 9H), 6.79 (t, $J = 7.4$ Hz, 9H), 6.64 (tt, $J = 7.3$, 1.5 Hz, 4H), 4.14 (s, 4H), 3.07 (t, $J = 5.3$ Hz, 4H), 1.14 (s, 9H). HRMS (ESI): *m/z* calcd for $C_{18}H_{25}CuN_3S^+$: 378.1060; found: 378.1062 $[M+L]^+$. Anal. calcd (%) for $C_{42}H_{45}BCuN_3S \cdot 0.6\ CH_2Cl_2$: C 68.29, H 6.22, N 5.61, found: C 68.15, H 6.11, N 5.62.

Research Article
doi.org/10.1002/ejic.202200626

[Cu(4)]PF_6: To a stirred solution of **4** (0.050 g, 0.14 mmol) in dichloromethane (2 mL) a solution of $[Cu(MeCN)_4]PF_6$ (0.052 g, 0.14 mmol) in dichloromethane (2 mL) was added dropwise. The solution was stirred over night at room temperature. Slow evaporation of the solvent led to yellow crystals that were suitable for X-ray structural characterization. Yield: 82.9 mg (0.113 mmol, 81%). HRMS (ESI): *m/z* calcd for $C_{21}H_{23}CuN_3S^+$: 412.0904; found: 412.0904 $[M+L]^+$; $C_{21}H_{23}ClCuN_3S^+$: 447.0592; found: 447.0594 $[M+L+Cl]^+$. Anal. calcd (%) for $C_{21}H_{23}CuF_6N_3PS \cdot 0.5\ CH_2Cl_2$: C 43.01, H 4.03, N 7.00, found: C 43.08, H 3.89, N 7.06.

[Cu(5)]BPh_4: To a stirred solution of **5** (0.021 g, 0.055 mmol) in dichloromethane (2 mL) a solution of $[Cu(MeCN)_4]PF_6$ (0.020 g, 0.054 mmol) in dichloromethane (2 mL) was added dropwise. After stirring for 2 h, solid $NaBPh_4$ (0.019 g, 0.054 mmol) was added and it was stirred over night at room temperature. The yellow solution was filtered and slow evaporation of the solvent led to colorless crystals that were suitable for X-ray structural characterization. Yield: 32.1 mg (0.0420 mmol, 78%).^{1}H NMR (700 MHz, acetone-*d6*): δ (ppm) = 8.61 (dt, J = 5.1, 1.5 Hz, 2H), 7.78 (td, J = 7.7, 1.7 Hz, 3H), 7.36 (dd, J = 7.6, 5.0 Hz, 5H), 7.21–7.19 (m, 7H), 7.04–6.99 (m, 3H), 6.78 (t, J = 7.4 Hz, 6H), 6.71–6.67 (m, 3H), 6.66–6.61 (m, 3H), 4.04 (s, 2H), 3.62 (s, 4H), 3.40 (s, 3H), 2.93 (dd, J = 6.8, 4.5 Hz, 2H), 2.85 (dd, J = 6.6, 4.7 Hz, 2H). HRMS (ESI): *m/z* calcd for $C_{22}H_{25}CuN_3OS^+$: 442.1009; found: 442.1006 $[M+L]^+$. Anal. calcd (%) for $C_{46}H_{45}BCuN_3OS \cdot 2.5\ CH_2Cl_2 \cdot CH_3CN$: C 59.72, H 5.26, N 5.52, found: C 59.24, H 5.08, N 5.52.

[Cu(6)]OTf: To a stirred solution of **6** (0.100 g, 0.295 mmol) in acetone (2 mL) a solution of $[Cu(MeCN)_4]OTf$ (0.109 g, 0.290 mmol) in acetone (2 mL) was added dropwise. The solution was stirred over night at room temperature. Slow evaporation of the solvent led to a yellow solid. Yield: 109 mg (0.197 mmol, 68%).^{1}H NMR (700 MHz, acetone-*d6*): δ (ppm) = 7.99 (t, J = 7.4 Hz, 5H), 7.43 (d, J = 1.9 Hz, 2H), 6.32 (dd, J = 3.2, 1.8 Hz, 2H), 6.29 (d, J = 3.2 Hz, 2H), 4.94 (s, 2H), 3.86 (s, 4H), 3.22 (s, 4H). HRMS (ESI): *m/z* calcd for $C_{19}H_{21}CuN_3OS^+$: 402.0696; found: 402.0699 $[M+L]^+$. Anal. calcd (%) for $C_{46}H_{45}BCuN_3OS$: C 43.51, H 3.83, N 7.61, found: C 43.48, H 3.78, N 7.42.

[Cu(7)]BPh_4: To a stirred solution of **7** (0.050 g, 0.17 mmol) in dichloromethane (2 mL) a solution of $[Cu(MeCN)_4]PF_6$ (0.065 g, 0.17 mmol) in dichloromethane (2 mL) was added dropwise. The mixture was stirred for 30 min at room temperature. An acetone solution (2 mL) of sodium tetraphenylborate (0.059 g, 0.17 mmol) was added to the reaction mixture and stirred at room temperature over night. The precipitated solid was filtrated, washed with diethyl ether and dried. Slow evaporation of the solvent led to colorless crystals that were suitable for X-ray structural characterization. Yield: 89.1 mg (0.133 mg, 77%). ^{1}H NMR (700 MHz, acetone-*d6*): δ (ppm) = 8.71 (d, J = 5.1 Hz, 2H), 7.93 (td, J = 7.7, 1.7 Hz, 2H), 7.53–7.47 (m, 4H), 7.36–7.30 (m, 8H), 6.94 (t, J = 7.5 Hz, 8H), 6.79 (tt, J = 7.2, 1.5 Hz, 4H), 4.04 (s, 4H), 3.12–2.96 (m, 3H), 2.76–2.64 (m, 3H), 2.33 (s, 3H). HRMS (ESI): *m/z* calcd for $C_{16}H_{21}CuN_3S^+$: 350.0747; found: 350.0752 $[M+L]^+$. Anal. calcd (%) for $C_{40}H_{41}BCuN_3S \cdot 0.5\ CH_2Cl_2$: C 68.26, H 5.94, N 5.90, found: C 68.49, H 6.02, N 6.36.

[Cu(8)]PF_6: To a stirred solution of **8** (0.050 g, 0.13 mmol) in acetone (2 mL) a solution of $[Cu(MeCN)_4]PF_6$ (0.050 g, 0.13 mmol) in acetone (2 mL) was added dropwise. The solution was stirred over night at room temperature. Slow evaporation of the solvent led to yellow crystals that were suitable for X-ray structural characterization. Yield: 68.0 mg (0.117 mmol, 88%). ^{1}H NMR (700 MHz, acetone-*d6*): δ (ppm) = 8.62 (d, J = 8.4 Hz, 2H), 8.41 (d, J = 8.5 Hz, 2H), 7.94 (d, J = 8.1 Hz, 2H), 7.90–7.83 (m, 2H), 7.59 (t, J = 7.59 Hz, 2H), 7.53 (d, J = 8.5 Hz, 2H), 4.60 (d, J = 17.4 Hz, 2H), 4.47 (d, J = 17.4 Hz, 2H), 3.16 (t, J = 5.6 Hz, 2H), 3.06 (t, J = 5.5 Hz, 2H), 1.73 (s, 3H). HRMS (ESI): *m/z* calcd for $C_{23}H_{23}CuN_3S^+$: 436.0904; found: 436.0904 $[M+L]^+$. Anal. calcd (%) for $C_{23}H_{23}CuF_6N_3PS$: C 47.46, H 3.98, N 7.22, found: C 46.75, H 3.85, N 7.02.

[Cu(9)]BPh_4: To a stirred solution of **9** (0.030 g, 0.076 mmol) in dichloromethane (2 mL) a solution of $[Cu(MeCN)_4]PF_6$ (0.028 g, 0.076 mmol) in dichloromethane (2 mL) was added dropwise. After stirring for 2 h, solid $NaBPh_4$ (0.026 g, 0.076 mmol) was added and it was stirred over night at room temperature. The yellow solution was filtered and slow evaporation of the solvent led to a yellow solid. Yield: 43.6 mg (0.0560 mmol, 74%). HRMS (ESI): *m/z* calcd for $C_{19}H_{27}CuN_3O_4S^+$: 456.101; found: 456.104 $[M+L]^+$; $C_{19}H_{27}ClCuN_3O_4S^+$: 491.0707; found: 491.0702 $[M+L+Cl]^+$. Anal. calcd (%) for $C_{43}H_{47}BCuN_3O_4S \cdot 4.5\ CH_2Cl_2 \cdot CH_3CN$: C 49.57 H 4.96 N 4.67, found: C 49.42, H 4.69, N 5.06.

[Cu(10)]PF_6: To a stirred solution of **10** (0.025 g, 0.058 mmol) in dichloromethane (2 mL) a solution of $[Cu(MeCN)_4]PF_6$ (0.021 g, 0.055 mmol) in dichloromethane (2 mL) was added dropwise. The solution was stirred over night at room temperature. Slow evaporation of the solvent led to a yellow solid. Yield: 24.6 mg (0.0390 mmol, 70%). HRMS (ESI): *m/z* calcd for $C_{24}H_{37}CuN_3O_2S^+$: 494.1897; found: 494.1895 $[M+L]^+$. Anal. calcd (%) for $C_{24}H_{37}CuF_6N_3O_2PS \cdot 0.5\ CH_2Cl_2$: C 43.11, H 5.61, N 6.16, found: C 43.27, H 5.71, N 6.08.

Oxygenation Reactions of Copper(I) Complexes: In the glove box, ca. 100 mg of the copper(I) complex were dissolved in 2 mL acetone (for −90 °C) or 2-MeTHF/THF (for −140 °C). Dioxygen was bubbled 5 min through the complex solution using a syringe needle.

Ozonolysis of Copper(I) Complexes: Ozonolysis was performed with the OZONOSAN PM 83 K. For the reactions with ozone and the copper(I) complexes absolute dry glassware was used. The complex solutions were prepared in a glove box. Ca. 100 mg of the copper complexes were dissolved in 2 mL acetone (for −90 °C) or 2-MeTHF/THF (for −140 °C). Ozone was bubbled 5 min through the complex solution with a special homebuilt glass cannula, which allowed bubbling ozone through the complex solution without any contact to the metal of a syringe needle.

Acknowledgements

We gratefully acknowledge support by the Justus-Liebig-Universität Gießen and the Deutsche Forschungsgemeinschaft for financial support (SS, SCHI 377/18-1). Furthermore, we would like to thank Stefan Schaub for his help in the laboratory with ozone handling. Open Access funding enabled and organized by Projekt DEAL.

Conflict of Interest

The authors declare no conflict of interest.

Data Availability Statement

The data that support the findings of this study are available from the corresponding author upon reasonable request.

Keywords: Copper · Dioxygen activation · Kinetics · Ozone · Stopped flow

[1] D. A. Quist, D. E. Diaz, J. J. Liu, K. D. Karlin, *J. Biol. Inorg. Chem.* **2017**, *22*, 253.
[2] a) K. A. Magnus, H. Ton-That, J. E. Carpenter, *Chem. Rev.* **1994**, *727*.
[3] a) K. D. Karlin, N. Wei, B. Jung, S. Kaderli, P. Niklaus, A. D. Zuberbuehler, *J. Am. Chem. Soc.* **1993**, *115*, 9506; b) J. P. Klinman, *Chem. Rev.* **1996**, *96*, 2541; c) J. P. Klinman, *J. Biol. Inorg. Chem.* **2006**, *281*, 3013; d) V. Gómez-Vidales, I. Castillo, *Eur. J. Inorg. Chem.* **2022**, in press: doi.org/10.1002/ejic.202100728.
[4] a) L. Q. Hatcher, K. D. Karlin, *J. Biol. Inorg. Chem.* **2004**, *9*, 669; b) E. A. Lewis, W. B. Tolman, *Chem. Rev.* **2004**, *104*, 1047; c) S. Schindler, *Eur. J. Inorg. Chem.* **2000**, *2000*, 2311; d) T. Osako, S. Nagatomo, Y. Tachi, T. Kitagawa, S. Itoh, *Angew. Chem.* **2002**, *114*, 4501.
[5] L. M. Mirica, X. Ottenwaelder, T. D. P. Stack, *Chem. Rev.* **2004**, *104*, 1013.
[6] S. T. Prigge, B. A. Eipper, R. E. Mains, L. M. Amzel, *Science* **2004**, *304*, 864.
[7] R. E. Cowley, L. Tian, E. I. Solomon, *Proc. Natl. Acad. Sci. USA* **2016**, *113*, 12035.
[8] S. Kim, J. W. Ginsbach, A. I. Billah, M. A. Siegler, C. D. Moore, E. I. Solomon, K. D. Karlin, *J. Am. Chem. Soc.* **2014**, *136*, 8063.
[9] S. Kim, J. Y. Lee, R. E. Cowley, J. W. Ginsbach, M. A. Siegler, E. I. Solomon, K. D. Karlin, *J. Am. Chem. Soc.* **2015**, *137*, 2796.
[10] J. Y. Lee, K. D. Karlin, *Curr. Opin. Chem. Biol.* **2015**, *25*, 184.
[11] R. R. Jacobson, Z. Tyeklar, A. Farooq, K. D. Karlin, S. Liu, J. Zubieta, *J. Am. Chem. Soc.* **1988**, *110*, 3690.
[12] L. Q. Hatcher, D.-H. Lee, M. A. Vance, A. E. Milligan, R. Sarangi, K. O. Hodgson, B. Hedman, E. I. Solomon, K. D. Karlin, *Inorg. Chem.* **2006**, *45*, 10055.
[13] M. Bhadra, W. J. Transue, H. Lim, R. E. Cowley, J. Y. C. Lee, M. A. Siegler, P. Josephs, G. Henkel, M. Lerch, S. Schindler et al., *J. Am. Chem. Soc.* **2021**, *143*, 3707.
[14] T. Hoppe, S. Schaub, J. Becker, C. Würtele, S. Schindler, *Angew. Chem.* **2013**, *52*, 870.
[15] T. Hoppe, P. Josephs, N. Kempf, C. Wölper, S. Schindler, A. Neuba, G. Henkel, *Z. Anorg. Allg. Chem.* **2013**, *639*, 1504.
[16] a) L. Zhou, D. Powell, K. M. Nicholas, *Inorg. Chem.* **2006**, *45*, 3840; b) G. Y. Park, Y. Lee, D.-H. Lee, J. S. Woertink, A. A. Narducci Sarjeant, E. I. Solomon, K. D. Karlin, *Chem. Commun.* **2010**, *46*, 91; c) T. Ohta, T. Tachiyama, K. Yoshizawa, T. Yamabe, T. Uchida, T. Kitagawa, *Inorg. Chem.* **2000**, *39*, 4358; d) Y. Lee, D.-H. Lee, G. Y. Park, H. R. Lucas, A. A. Narducci Sarjeant, M. T. Kieber-Emmons, M. A. Vance, A. E. Milligan, E. I. Solomon, K. D. Karlin, *Inorg. Chem.* **2010**, *49*, 8873.
[17] E. A. Ambundo, M.-V. Deydier, A. J. Grall, N. Aguera-Vega, L. T. Dressel, T. H. Cooper, M. J. Heeg, L. A. Ochrymowycz, D. B. Rorabacher, *Inorg. Chem.* **1999**, *38*, 4233.
[18] D.-H. Lee, L. Q. Hatcher, M. A. Vance, R. Sarangi, A. E. Milligan, A. A. N. Sarjeant, C. D. Incarvito, A. L. Rheingold, K. O. Hodgson, B. Hedman et al., *Inorg. Chem.* **2007**, *46*, 6056.
[19] P. Josephs, *dissertation* **2017**, University Paderborn.
[20] M. Schatz, V. Raab, S. P. Foxon, G. Brehm, S. Schneider, M. Reiher, M. C. Holthausen, J. Sundermeyer, S. Schindler, *Angew. Chem.* **2004**, *43*, 4360.
[21] T. Rotärmel, J. Becker, S. Schindler, *Faraday Discuss.* **2022**, *234*, 70.
[22] H. Sterckx, B. Morel, B. U. W. Maes, *Angew. Chem.* **2019**, *58*, 7946.
[23] a) N. W. Aboelella, B. F. Gherman, L. M. R. Hill, J. T. York, N. Holm, V. G. Young, C. J. Cramer, W. B. Tolman, *J. Am. Chem. Soc.* **2006**, *128*, 3445; b) I. Castillo, V. M. Ugalde-Saldívar, L. A. Rodríguez Solano, B. N. Sánchez Eguía, E. Zeglio, E. Nordlander, *Dalton Trans.* **2012**, *41*, 9394; c) M. Gennari, M. Tegoni, M. Lanfranchi, M. A. Pellinghelli, M. Giannetto, L. Marchiò, *Inorg. Chem.* **2008**, *47*, 2223.
[24] a) M. Wern, T. Hoppe, J. Becker, S. Zahn, D. Mollenhauer, S. Schindler, *Eur. J. Inorg. Chem.* **2016**, *2016*, 3384; b) M. E. Helton, D. Maiti, L. N. Zakharov, A. L. Rheingold, J. A. Porco, K. D. Karlin, *Angew. Chem.* **2006**, *45*, 1138; c) D. Maiti, J. S. Woertink, M. A. Vance, A. E. Milligan, A. A. N. Sarjeant, E. I. Solomon, K. D. Karlin, *J. Am. Chem. Soc.* **2007**, *129*, 8882.
[25] B.-J. Liaw, T. S. Lobana, Y.-W. Lin, J.-C. Wang, C. W. Liu, *Inorg. Chem.* **2005**, *44*, 9921.
[26] a) E. A. Ambundo, M. V. Deydier, L. A. Ochrymowycz, D. B. Rorabacher, *Inorg. Chem.* **2000**, *39*, 1171; b) F. Jiang, M. A. Siegler, E. Bouwman, *Inorg. Chim. Acta* **2019**, *486*, 135; c) E. C. M. Ording-Wenker, M. A. Siegler, M. Lutz, E. Bouwman, *Dalton Trans.* **2015**, *44*, 12196.
[27] a) M. Weitzer, S. Schindler, G. Brehm, S. Schneider, E. Hörmann, B. Jung, S. Kaderli, A. D. Zuberbühler, *Inorg. Chem.* **2003**, *42*, 1800; b) C. X. Zhang, S. Kaderli, M. Costas, E.-I. Kim, Y.-M. Neuhold, K. D. Karlin, A. D. Zuberbühler, *Inorg. Chem.* **2003**, *42*, 1807.
[28] a) A. Hoffmann, M. Wern, T. Hoppe, M. Witte, R. Haase, P. Liebhäuser, J. Glatthaar, S. Herres-Pawlis, S. Schindler, *Eur. J. Inorg. Chem.* **2016**, *2016*, 4744; b) M. Lerch, M. Weitzer, T.-D. J. Stumpf, L. Laurini, A. Hoffmann, J. Becker, A. Miska, R. Göttlich, S. Herres-Pawlis, S. Schindler, *Eur. J. Inorg. Chem.* **2020**, 3143.

Manuscript received: October 7, 2022
Revised manuscript received: November 25, 2022
Accepted manuscript online: November 27, 2022